Automatic Derivation of Equivalent Circuits for General Microstrip Interconnection Discontinuities

Guy Coen, *Student Member, IEEE,* Daniel De Zutter, *Member, IEEE,* and Niels Faché, *Member, IEEE*

***Abstract*—The techniques presented in this paper allow one to automatically derive equivalent LC-networks for general lossless microstrip interconnection discontinuities. The method is completely based on physical considerations and does not involve any fitting procedure. The technique is quite fast, and the resulting networks are closely related to the physical structure. Due to the fact that we only use lumped passive circuit elements, the structures under consideration are assumed to be small as compared to the electrical wavelength. The extension of our technique to multilayered planar structures with vias is possible. It is also possible to deal with lossy dielectrics, finite conductivity metallizations, and radiation. The main application area of our technique is the modeling of interconnection discontinuities in high speed digital circuits.**

I. Introduction

In MICROWAVE modeling, it is common practice to perform all calculations in the frequency domain. Most modeling tools currently on the market for the computer aided analysis and design of microwave circuits are based on S-parameter models for the subparts of the structures under consideration. In the literature, there are a large number of accurate and efficient modeling techniques for the derivation of these S-parameter models.

In high speed digital analysis and synthesis, both time and frequency domain calculations are used. The most generally used computer aided modeling tool for digital applications is SPICE. In contrast to the wide availability of S-parameter models for interconnection discontinuities, there is a lack of accurate and efficient SPICE-models for general interconnection discontinuities. The most desired models are RLC-models, since these can be most efficiently handled by SPICE.

In the past, a number of techniques have been developed for the derivation of RLC-models for planar interconnection discontinuities. One of the earliest techniques for the analysis of planar discontinuities was the planar waveguide model [1], [2]. Based on this approximation, techniques were developed to derive RLC-models for a large number of frequently used planar interconnection discontinuities [3]–[5]. A variation of this technique is the planar-lumped model [6], [7]. In this case, the planar waveguide models are used for every metal patch, while the fringing effects in the gaps are modeled with lumped circuits.

Manuscript received April 10, 1995, revised March 20, 1996

G. Coen and D. De Zutter are with the Department of Information Technology, University of Ghent, Belgium, 9000 Ghent, Belgium. G Coen and D. De Zutter are also with the National Fund for Scientific Research of Belgium.

N. Faché is with HP-EEsof, 9000 Ghent, Belgium.

Publisher Item Identifier S 0018-9480(96)04699-6.

Another approach to calculate lumped RLC-circuits for planar structures are the so-called matrix methods. This approach is purely static and models only excess charges and currents with a lumped model. A general description of this technique is given in [8]–[10]. The calculation of capacitors with matrix methods is given in [11]–[14]. The calculation of inductors is treated in [15]–[18]. These matrix methods are based on the method of moments [19] (MoM). It was shown experimentally in [20] that these matrix methods were an improvement as compared to the planar waveguide models. The matrix methods described above are purely static. They deal either with the capacitive effect or with the inductive one, but cannot describe a combined effect.

A common characteristic of all the techniques described above is that the lumped models represent excess effects. One locates a number of transmission lines in the structure, and puts a reference plane at the end of these transmission lines, or at a point where they all meet. The transmission lines are then represented by a two-dimensional (2-D)-based model, whereas the excess effects are modeled using lumped elements. The advantage of this approach is that the structure represented by the lumped element model is certainly small as compared to the wavelength. However, a drawback of the technique is the fact that one must be able to locate transmission lines in the structure. This makes it less interesting for the modeling of very general interconnection discontinuities.

Another approach for the derivation of SPICE-models for interconnection structures is the PEEC-method [21]–[26]. This technique has the advantage that it can handle very general interconnection discontinuities (even general three-dimensional (3-D) structures such as connectors) in a broad frequency range. If retardation effects are taken into account, the (r)-PEEC models consist of RLC-elements, as well as time delayed voltage or current dependent sources. A disadvantage is the complexity of the resulting networks when a dense mesh is required to represent the structure under consideration. The authors of the (r)-PEEC method also developed a special network solution technique for dealing with very large circuits, called the modified nodal approach [27].

In this paper a new technique is presented that combines the generality of the (r)-PEEC method and the simplicity of parallel plate models. Furthermore, our technique is such that the models resulting from it can easily be interpreted physically. The compromise that we have adopted is that the models derived from our technique are only valid in the frequency range where the structure under consideration is small as compared to the wavelength. Our approach results in

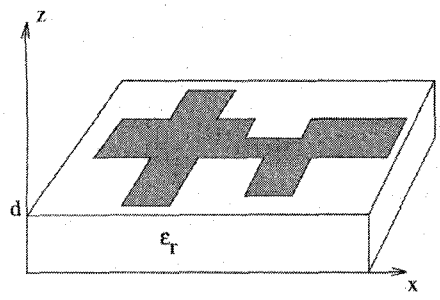

Fig. 1. Microstrip structure.

lumped element networks that represent the whole structure, not just excess effects. In contrast to the matrix methods mentioned above, our technique deals with both inductive and capacitive effects at the same time.

II. General Outline of the Equivalent Network Generation Procedure

The structures under consideration in this paper are general multiport microstrip interconnection discontinuities. The substrate is assumed to be isotropic and lossless. The metallization layers are considered to be infinitely thin (Fig. 1). The extension to multilayered planar circuits with vias is mainly an implementation issue, and poses no great additional difficulties. We are currently extending the technique so that losses can also be taken into account.

At the starting point of our method we only need the substrate properties, the polygonal shape of the metallization pattern and the bandwidth over which the model is to be valid. Optionally, the overall precision of the network model can also be specified. The rest of the procedure is completely automated.

The basis of our technique is a (MoM) [19] solution of an appropriately chosen mixed potential integral equation [2] (MPIE). First, a mesh of rectangles and triangles is fitted onto the polygonal shape of the metallization pattern [28]. Corresponding with this mesh, we can calculate the partial elements description (PED) of the structure, as described in Section III. Then, we trace and eliminate the redundancy in the mesh, as explained in Section IV. Next, the topology of the equivalent network and the impedance matrix are calculated.

In this paper, we shall not go into details about the meshing of the polygonal shape of the structure under consideration, which is described in [29]. In Section V we shall briefly indicate how we calculate the element values in the reduced network. Finally, in Section VI, we shall illustrate the techniques presented in this paper by means of an example.

III. Partial Element Description

In this section, we shall derive a circuit description for microstrip circuits that is very analogous to the PEEC-description that Ruehli introduced for general 3-D structures. However, a PEEC-network is a PED of a general 3-D structure, corresponding to the particular mesh that Ruehli introduced. The networks derived here are for microstrip structures, and the mesh used is the one introduced in [29]. Another important

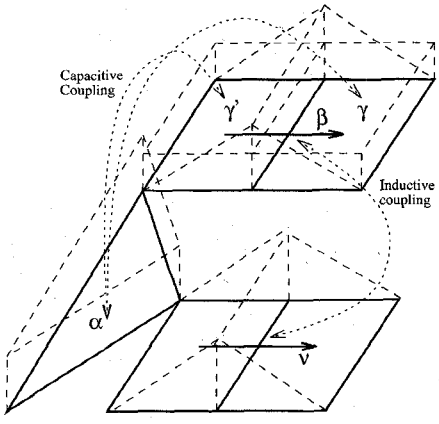

Fig. 2. Base for partial element description.

difference lies in the final description of the partial elements: Ruehli uses delayed dependent sources, we do not. In order to avoid confusion with Ruehli's technique, we have chosen to use the term PED for the partial element network derived below.

We start from the following mixed potential integral equation (MPIE) for a microstrip structure [29]

$$\overline{0} = -j\omega\frac{\mu_0}{4\pi}\int_S dS'\overline{J}(x', y')G_m(\rho, z, d) - \frac{1}{4\pi\epsilon_0}\nabla_t\int_S dS'\rho(x', y')G_e(\rho, z, d) \quad (1)$$

G_e and G_m are the electric and magnetic Green's functions, respectively, [29]. The microstrip structure is located at $z' = d$ (Fig. 1). Now, instead of transforming the charge density in the above equation into a current density, in order to obtain an integral equation in the current density alone, we introduce a separate, yet consistent model for charge and current density. The current density is approximated using a linear combination of rooftop basis functions as in [29], whereas the charge density is approximated using pulse basis functions (i.e., piecewise constant over each mesh cell), as illustrated in Fig. 2. This is exactly the charge density approximation that corresponds to a rooftop approximation of the current density. The difference however is that, at this point, we do not yet use the charge continuity equation

$$\nabla\cdot\overline{J} + j\omega\rho = 0. \quad (2)$$

The approximations mentioned above can be stated as follows:

$$\begin{cases}\overline{J}(\overline{r}) \approx \sum\limits_{\nu=1}^{N_S}\frac{I_\nu}{l_\nu}\overline{H}_\nu(\overline{r}) \\ \rho(\overline{r}) \approx \sum\limits_{\alpha=1}^{N_C}\frac{Q_\alpha}{S_\alpha}p_\alpha(\overline{r}).\end{cases} \quad (3)$$

In this equation, $\overline{J}(\overline{r})$ and $\rho(\overline{r})$ are the current density and charge density, respectively. I_ν and ℓ_ν, respectively, are the current through and the length of mesh side ν. $\overline{H}_\beta$ is given by (18) in [29].

Furthermore, Q_α is the total charge on and S_α the area of mesh cell α. The function $p_\alpha(\overline{r})$ is one on mesh cell α, and

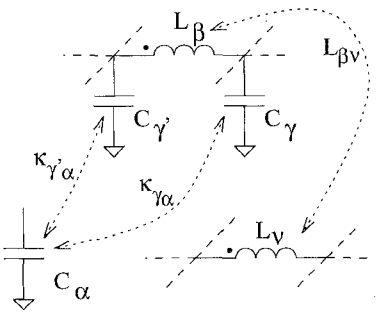

Fig. 3. Partial element description.

zero elsewhere. N_S is the total number of mesh sides, and N_C the total number of mesh cells.

If we substitute the approximations (3) in the MPIE (1) and apply Galerkin weighting, the integral equation is discretized to

$$0 = j\omega\frac{\mu_0}{4\pi}\sum_{\nu=1}^{N_S} I_\nu \int_{S_\beta} dS\frac{\overline{H}_\beta}{l_\beta}\cdot\int_{S_\nu} dS'\frac{\overline{H}_\nu}{l_\nu}G_m + \frac{1}{4\pi\epsilon_0}\sum_{\alpha=1}^{N_C}\frac{Q_\alpha}{S_\alpha S_\gamma}\int_{S_\gamma} dS\int_{S_\alpha} dS'G_e - \frac{1}{4\pi\epsilon_0}\sum_{\alpha=1}^{N_C}\frac{Q_\alpha}{S_\alpha S_{\gamma'}}\int_{S_{\gamma'}} dS\int_{S_\alpha} dS'G_e. \quad (4)$$

Now if we introduce the following notations:

$$\begin{cases} L_{\beta\nu} = \frac{\mu_0}{4\pi}\frac{1}{l_\beta l_\nu}\int_{S_\beta} dS\overline{H}_\beta\cdot\int_{S_\nu} dS'\overline{H}_\nu G_m \\ \kappa_{\gamma\alpha} = \frac{1}{4\pi\epsilon_0}\frac{1}{S_\alpha S_\gamma}\int_{S_\beta} dS\int_{S_\alpha} dS'G_e \end{cases} \quad (5)$$

(4) can be rewritten as

$$0 = \sum_{\nu=1}^{N_S} j\omega L_{\beta\nu}I_\nu + \sum_{\alpha=1}^{N_C}\kappa_{\gamma\alpha}Q_\alpha - \sum_{\alpha=1}^{N_C}\kappa_{\gamma'\alpha}Q_\alpha. \quad (6)$$

This equation can be interpreted as the Kirchhoff voltage law in an elementary loop consisting of one inductor L_β and two capacitors C_γ and $C_{\gamma'}$, as illustrated in Fig. 3. Equation (6) can be written down for each current carrying mesh side $\beta = 1, \cdots, N_S$. The inductor L_β comes from the rooftop on mesh side β. The capacitors C_γ and $C_{\gamma'}$ come from the pulse basis functions on mesh cells γ and γ' (Figs. 2 and 3). As one can see, we can associate an inductor with each current carrying mesh side ν, and a capacitor with each mesh cell α.

Equation (6) also shows that, in order for our network to correspond to the physical situation, we must assume that each inductor L_β is mutually coupled to all the other inductors L_ν in the circuit. Also, each capacitor C_γ must be assumed to couple with all the other capacitors C_α. This is also illustrated in Figs. 2 and 3.

It is at this point that the charge continuity equation (2) is taken into account, namely as Kirchhof's current law in the network defined by (6).

In the rest of this paper, we shall refer to the network just described as the PED of the structure under consideration. The matrices κ and L describe the capacitive and inductive couplings, respectively. From now on, we shall refer to them as the partial element matrices (PEM).

IV. Mesh Reduction

Suppose we know the current through each mesh side and the charge on each mesh cell, corresponding to a given excitation of the structure under consideration. With this information, and the partial element matrices, we can calculate the electric energy density associated with each mesh cell, ϵ_α^e and the magnetic energy density associated with each mesh side, ϵ_ν^m

$$\epsilon_\alpha^e = \frac{1}{2S_\alpha}\sum_{\gamma=1}^{C} Q_\alpha^*\kappa_{\alpha\gamma}Q_\gamma \quad (7)$$

$$\epsilon_\nu^m = \frac{1}{2l_\nu}\sum_{\beta=1}^{S} I_\nu^* L_{\nu\beta}I_\beta \quad (8)$$

where S_α is the area of mesh cell α, and l_ν the length of mesh side ν.

Now, if the magnetic energy associated with a mesh side is small as compared to the electric energy density associated with the neighboring mesh cells, then the area of the structure consisting of these mesh cells can be considered to be dominantly capacitive, and the mesh side (i.e., the induction at this point) will have only a minor importance. Now, if we set forth a cut-off value δ, we can say that a mesh side ν will be redundant if

$$\frac{\epsilon_\nu^m}{\epsilon_\nu^e} < \delta \quad (9)$$

where ϵ_ν^m and ϵ_ν^e are the magnetic and electric energy densities associated with side ν (and its neighboring mesh cells), respectively. The smaller we choose the value δ, the more dense the mesh will be after our reduction step.

This process can be repeated for a number of "representative excitations." A mesh side will be essential if it turns out to be essential for any one of those excitations. An alternative is to apply (9) to the mean energy densities resulting from all the representative excitations. This is the approach we have followed for the example in Section VI. One possible choice for these "representative excitations" is to use N_P of them, N_P being the number of ports in the structure. In excitation i, port i is excited with a Norton source, while all the ports are terminated in their characteristic impedances.

A. Evaluation

It is true that the criterion we propose here is not the only possibility. In fact, we have investigated and compared a lot of alternatives. The criterion that we suggest in this paper is the one that gave the best results. It also has a number of interesting properties, as we shall illustrate in this section.

Consider the canonical case of a piece of microstrip transmission line. It is commonly known that at sufficiently low frequencies, the longitudinal current density is a couple of orders of magnitude larger than the transverse current density [30]. One could propose a criterion to discriminate between dominantly capacitive and dominantly inductive behavior, based on this knowledge alone. For the canonical case considered, and at sufficiently low frequencies, this would give

good results, because in that case, the "voltage" induced by the transverse current is also a lot smaller than that induced by the longitudinal current. However, in a more general case, we could have situations where a smaller current density in some direction gives rise to a larger "voltage difference" than a larger current density in some other direction, because the induction in the former direction is much larger than that in the latter. This effect would not be captured by that simple criterion. It is captured however, by our criterion (9).

Let us stick with our canonical case. Suppose we used three or more cells in the transverse direction, and consider a number of mesh sides with the same longitudinal coordinate. Due to the fact that the longitudinal current density is larger near the edges of the strip [30], the simple criterion from above would find mesh sides near the edges more important than those in the center of the strip, which is not very logical. The energy density ratio that we use has the interesting property that it is almost equal for all the mesh sides mentioned above. So, if one of those mesh sides is found to be redundant, they will all be eliminated, which is essential for a "clean" elimination of the transverse direction.

V. Element Values

A. Introduction

Our mesh reduction technique would be of little use if one would not be able to calculate the circuit elements corresponding to the reduced mesh. Our first step is to separate the inductive and capacitive subnetworks. The capacitive subnetwork describes the electric energy distribution, while the inductive subnetwork describes the inductive energy distribution.

The idea is that we calculate the element values in each subnetwork, and then put the reduced networks back together. In order for this to be possible, we shall have to take some precautions.

In the mesh reduction step, the elimination of reduced mesh sides according to (9) leads to a subdivision of the structure into a number of surface patches. Each patch consists of a number of mesh cells used in the solution of (1).

Within each patch, one mesh cell is chosen to represent that patch. The node corresponding with that mesh cell in the PED becomes a node for the reduced network as well. From now on, we shall call these the internal nodes. They represent the information that we need in order to be able to put the two separately reduced subnetworks back together. The choice of the representative mesh cells is very important. We shall discuss this issue later on in this paper. The reduced network also has one node per (external) port. These will be called external nodes.

Now let us define "neighboring nodes." Two nodes are neighboring if they correspond with neighboring patches, or with a patch and its neighboring (external) port.

The reduced network has two kinds of network elements. Between each node corresponding with a patch and the ground node, we have a capacitor. Between each two neighboring nodes, we have an inductor. The mutual couplings are also retained.

The reason why we can approximately treat the two subnetworks separately is twofold. First of all, there is no mutual coupling between elements in the capacitive subnetwork, and elements in the inductive subnetwork. The interaction follows from the interconnection of the two subnetworks. The second reason was in fact already put forward in Section IV. At eliminated nodes of the PED, the interaction is negligible due to the criteria used in the mesh reduction procedure. At the remaining nodes, the interaction is taken into account when the two reduced subnetworks are reconnected.

B. Choosing the Representing Mesh Cells

The particular choice of a representing mesh cell in each patch does not influence the topology of the reduced network, only the element values. It is a rather delicate matter. We have used a stability criterion, based on energy considerations.

First of all, we attribute a "force" to each mesh cell α. This "force" of each mesh cell is given by the formula

$$\overline{F_\alpha} = \sum_s R_s \overline{u}_s \tag{10}$$

where the summation is done over all the sides (three for a triangle, four for a rectangle) of the mesh cell. In this formula, R_s is the ratio of the magnetic to the electric energy density for side s (the electric energy density is calculated for the mesh cells that have the common mesh side s). The unit vector $\overline{u_s}$ is orthogonal to side s of the mesh cell, and directed along the current through that mesh side. The representing mesh cell within each patch is the mesh cell for which the amplitude of this "force" is minimum within the considered patch. This is the most "stable" mesh cell within the patch.

Again, the criterion for choosing the representing mesh cells is far from unique. It is again one of the many possibilities that we have investigated, and which gave the best results.

C. Calculation of the Complex Impedance Matrix

We shall not go into details here about the calculation procedures. Instead, we shall restrict ourselves to a description of the underlying principles. We shall describe the principles by means of the simple example of a two port with a rectangular shape with a mesh consisting of 18 cells, as depicted in Figs. 4 and 5.

D. Calculation of Inductances

For the calculation of the inductors in the reduced network (and their mutual couplings), we refer to Fig. 4. The mesh sides represented by dotted lines were found to be redundant by the mesh reduction procedure. The three remaining mesh sides (middle full line in Fig. 4) divide the structure into two equal patches. The representing mesh cells within these patches were assigned internal node labels B and C. There are also two external nodes at the (external) ports, labeled A and D.

We consider the inductive PED network to be inside a black box. Our only means of access to it are what we call internal ports. An internal port (IP) is defined for each pair of

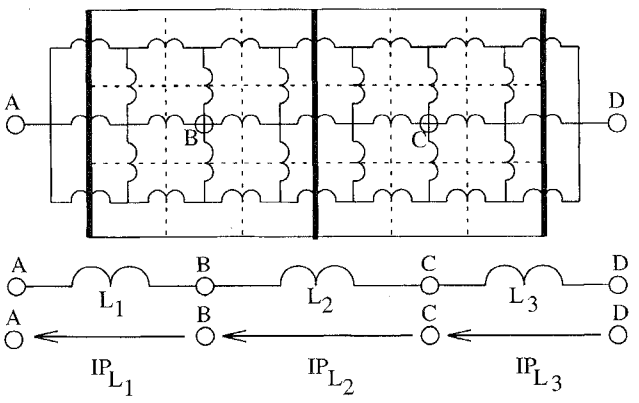

Fig. 4. Calculation of inductances.

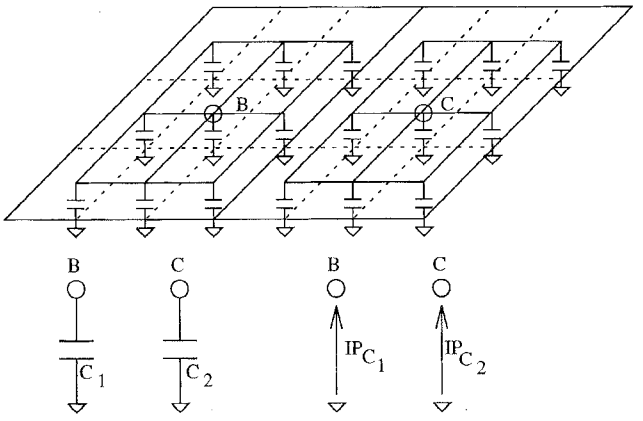

Fig. 5. Calculation of capacitors.

neighboring nodes (see IP_{L_1}, IP_{L_2}, and IP_{L_3} in Fig. 4). The positions of these internal ports correspond with those of the inductors in the reduced network (L_1, L_2, and L_3 in Fig. 4).

As the considered network contains only inductors, the resulting impedance matrix of the reduced network will be of the form

$$V = j\omega \mathcal{L} I \tag{11}$$

where V is the vector of internal port voltages, I is the vector of internal port currents, and $\mathcal{L}$ is the inductance matrix of the reduced network that we are looking for. The underlying principle for the calculation of the $\mathcal{L}$-matrix is quite straightforward. Apply an ideal current source I_j to internal port IP_{L_j}, leaving all the other internal ports open. Now measure the resulting voltage drop V_i over each internal port IP_{L_i}. We then have

$$\mathcal{L}_{ij} = \frac{V_i}{j\omega I_j}. \tag{12}$$

We have also developed a technique to perform the calculations just described quite easily. It is based on network diakoptics [31], but we shall not go into further detail upon that subject in this paper.

E. Calculation of Capacitors

For the calculation of the capacitors (and their mutual couplings) in the reduced network, the left out PED inductors within a patch are replaced by short circuits. The PED inductors that cross patches are replaced by open circuits (Fig. 5). The internal ports are now between an internal node and the ground node, as illustrated in Fig. 5. The positions of the two internal ports IP_{C_1} and IP_{C_2} correspond with those of the capacitors C_1 and C_2 in the reduced network. The rest of the procedure is very analogous to the one described in the previous section. There is one extra complication, namely the transformation of mutual capacitive couplings into capacitors. This will be described in the example in Section VI.

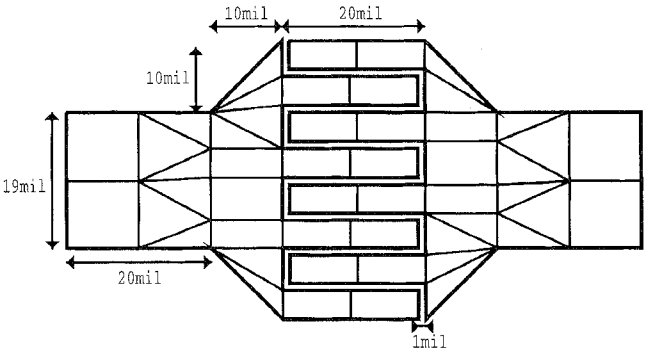

Fig. 6. Interdigital capacitor and dense mesh.

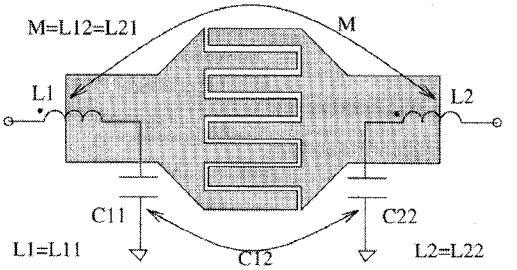

Fig. 7. Derived network.

VI. Example

As an example, we have taken the rather general and practical case of an interdigital capacitor. The substrate used is a lossless alumina substrate with $\epsilon_r = 9.6$ and a thickness of 25 mil. The metallization layer is infinitely thin and perfectly conducting. The dimensions and the mesh used are given in Fig. 6. We have requested a bandwidth of 5 GHz.

For this particular case, our mesh reduction scheme eliminated all internal sides. The resulting equivalent network, automatically derived with our method in a few seconds, is given in Fig. 7. The reader can easily see the physical meaning of each circuit component.

Mutual inductive couplings are well known components, but mutually coupled capacitors are not. We can however transform any capacitance matrix into a network of capacitors only, using standard techniques [32]. If we set

$$C_1 = C_{11} + C_{12} \tag{13}$$

$$C_2 = C_{22} + C_{12} \tag{14}$$

$$C_3 = -C_{12} \tag{15}$$

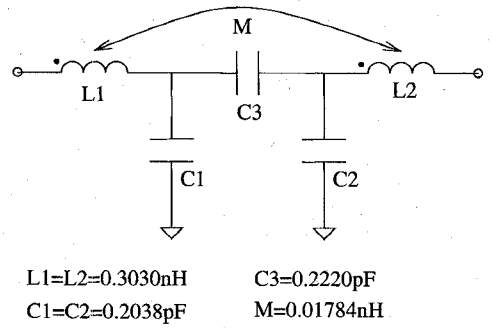

Fig. 8. Equivalent network.

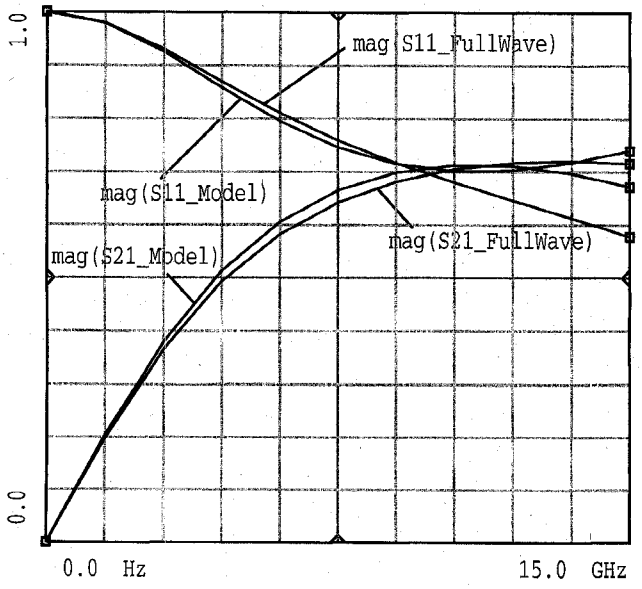

Fig. 9. Comparison with full wave analysis.

we get the final equivalent network, as depicted in Fig. 8. The element values are also given. In Fig. 9, we have compared the S-parameters (reference impedance 50 Ohm at both ports) obtained from our network, with those calculated using a full-wave MoM analysis of the structure. In order to get consistent results, we have used a Norton circuit excitation and lumped resistor terminations for both the full-wave MoM simulation and the simulation of our equivalent network. We see that we have a very good correspondence up to about 10 GHz.

We have already noted that we have set the requested bandwidth for the model to 5 GHz in this example. This made it possible to derive a network of the simplicity of that in Fig. 8. If we set the requested bandwidth to 15 GHz, our technique automatically adds extra networks for the modeling of the fingers in the interdigital capacitor. So, we can say that the deterioration of the quality of our model above 10 Ghz is due to the fact that our simple network no longer suffices. Our technique not only detects this, but is also capable of providing a more complex equivalent model if a larger bandwidth is needed.

VII. Conclusion

In this paper, we have described a technique which allows the fully automatic derivation of lumped element equivalent networks for general microstrip interconnection discontinuities. The networks are obtained on a physical basis, and do not require any fitting techniques. The method is very versatile and fast, and results in equivalent circuits that are very closely related to the physical structure.

References

[1] G. Kompa and R. Mehran, "Planar waveguide model for calculating microstrip components," *Electron. Lett.*, vol. 11, no. 19, pp. 459–460, Sept. 1975.
[2] T. Itoh, *Numerical Techniques for Microwave and Millimeter-Wave Passive Structures*. New York: Wiley, 1989.
[3] A. A. Oliner, "Equivalent circuits for discontinuities in balanced strip transmission line," *IRE Trans. Microwave Theory Tech.*, vol. MTT-3, pp. 134–143, Mar. 1955.
[4] ——, "Equivalent circuits for small symmetric longitudinal apertures and obstacles," *IRE Trans. Microwave Theory Tech.*, vol. MTT-8, pp. 72–80, Jan. 1960.
[5] K. S. Rao and V. M. Phandharipande, "Equivalent network for an aperture in the center conductor of microstrip line," *IEEE Trans. Microwave Theory Tech.*, vol. 39, no. 1, pp. 149–151, Jan. 1991.
[6] A. Sabban and K. C. Gupta, "Characterization of radiation loss from microstrip discontinuities using a multiport network modeling approach," *IEEE Trans. Microwave Theory Tech.*, vol. 39, no. 4, pp. 705–712, Apr. 1991.
[7] ——, "A planar-lumped model for coupled microstrip lines and discontinuities," *IEEE Trans. Microwave Theory Tech.*, vol. 40, no. 2, pp. 245–252, Feb. 1992.
[8] A. Farrar and A. T. Adams, "Matrix methods for field problems," *IEEE Proc.*, vol. 55, pp. 136–149, Feb. 1967.
[9] ——, "Matrix methods for microstrip three-dimensional problems," *IEEE Trans. Microwave Theory Tech.*, vol. MTT-20, no. 8, pp. 497–504, Aug. 1972.
[10] ——, "Computation of lumped microstrip capacitancies by matrix methods—rectangular sections," *IEEE Trans. Microwave Theory Tech.*, vol. MTT-19, no. 5, pp. 495–497, May 1971.
[11] P. Silvester and P. Benedek, "Equivalent capacitances of microstrip open circuits," *IEEE Trans. Microwave Theory Tech.*, vol. MTT-20, no. 8, pp. 511–516, Aug. 1972.
[12] P. Benedek and P. Silvester, "Capacitance of parallel rectangular plates separated by a dielectric sheet," *IEEE Trans. Microwave Theory Tech.*, vol. MTT-20, no. 8, pp. 504–510, Aug. 1972.
[13] ——, "Microstrip discontinuity capacitances for right-angle bends, t junctions, and crossings," *IEEE Trans. Microwave Theory Tech.*, vol. MTT-21, no. 5, pp. 341–346, May 1973.
[14] ——, "Correction to microstrip discontinuity capacitances for right-angle bends, t junctions, and crossings," *IEEE Trans. Microwave Theory and Tech.*, p. 456, May 1975.
[15] A. Gopinath and P. Silvester, "Calculation of inductance of finitelength strips and its variation with frequency," *IEEE Trans. Microwave Theory Tech.*, vol. MTT-21, no. 6, pp. 380–386, June 1973.
[16] A. Gopinath and B. Easter, "Moment method of calculating discontinuity inductance of microstrip right-angled bends," *IEEE Trans. Microwave Theory Tech.*, pp. 880–883, Oct. 1974.
[17] A. F. Thompson and A. Gopinath, "Calculation of microstrip discontinuity inductances," *IEEE Trans. Microwave Theory Tech.*, vol. MTT-23, no. 8, pp. 648–655, Aug. 1975.
[18] A. Gopinath, A. F. Thompson, and I. M. Stephenson, "Equivalent circuit parameters of microstrip step change in width and cross junctions," *IEEE Trans. Microwave Theory Tech.*, pp. 142–144, Mar. 1976.
[19] R. F. Harrington, *Field Computation by MoMent Methods*. New York: Macmillan, 1968.
[20] B. Easter, "The equivalent circuit of some microstrip discontinuities," *IEEE Trans. Microwave Theory Tech.*, vol. MTT-23, no. 8, pp. 655–660, Aug. 1975.
[21] H. Heeb *et al.*, "Three-dimensional interconnect analysis using partial element equivalent circuits," *IEEE Trans. Circuits Syst. I*, vol. 39, no. 11, pp. 974–976, Nov. 1992.
[22] R.-B. Wu *et al.*, "Inductance and resistance computations for three dimensional multiconductor interconnection structures," *IEEE Trans. Microwave Theory Tech.*, vol. 40, no. 2, pp. 263–267, Feb. 1992.
[23] A. E. Ruehli, "Circuit models for three-dimensional geometries including dielectrics," *IEEE Trans. Microwave Theory Tech.*, vol. 40, no. 7, pp. 1507–1512, 1992.

[24] P. A. Brennan *et al.*, "Three-dimensional inductance computations with partial element equivalent circuits," *IBM J. Res. Develop.*, vol. 23, no. 6, Nov. 1979.
[25] A. E. Ruehli and P. A. Brennan, "Capacitance models for integrated circuit metallization wires," *IEEE J. Solid State Circ.*, vol. SC-10, pp. 530–536, 1975.
[26] ——, "Accurate metallization capacitances for integrated circuits and packages," *IEEE J. Solid State Circ.*, vol. SSC-8, pp. 289–290, 1973.
[27] C. W. Ho, A. E. Ruehli, and P. A. Brennan, "The modified nodal approach to network analysis," *IEEE Trans. Circuits Syst. I*, vol. CAS1-22, pp. 504–509, Jan. 1975.
[28] HP-EEsof, *HP-MoMentum Version A.02.00*, Apr. 1995.
[29] D. C. Chang *et al.*, "Electromagnetic modeling of passive circuit elements in mmic," *IEEE Trans. Microwave Theory Tech.*, vol. 44, pp. 1741–1747, Sept. 1992.
[30] Guy Coen *et al.*, "Comparison between two sets of basis functions for the current modeling in the galerkin spectral domain solution for microstrip," *IEEE Trans. Microwave Theory Tech.*, vol. 42, no. 3, pp. 505–513, Mar. 1994.
[31] H. H. Happ, *Diakoptics and Networks*. New York: Academic Press, 1971.
[32] Guy Coen *et al.*, "Automatic equivalent discrete distributed circuit generated for microstrip interconnection discontinuities," in *IEEE Int. Symp. Antennas Propagat.*, June 1994, pp. 1702–1705.

Guy Coen (S'93) was born July 16, 1969, in Aalst, Belgium. He received the degree in electrical engineering from the University of Ghent, Belgium, in 1992. He is currently working toward the Ph.D. degree in electrical engineering at the Department of Information Technology (Intec) of the same university.

His research focuses on the modeling of high-frequency and high-speed interconnections.

Daniel De Zutter (M'92) was born November 8, 1953, in Eeklo, Belgium. He received the degree in electrical engineering from the University of Ghent in July 1976. In October 1981, he obtained the Ph.D. degree there and in the spring of 1984 he completed a thesis leading to the degree equivalent to the French Aggrégation or the German Habilitation.

From 1976 to 1984, he was a Research and Teaching Assistant in the Department of Information Technology (Intec) at the same university. He is now a Professor at Ghent University and Research Director at the National Science Foundation of Belgium. Most of his earlier scientific work dealt with the electrodynamics of moving media, with emphasis on the Doppler effect and Lorentz forces. His research now focuses on all aspects of circuit and electromagnetic modeling of high speed and high-frequency interconnections and on EMC and EMI topics. He has contributed to more than 50 journal papers.

In 1990 he was elected as a member of the Electromagnetics Society.

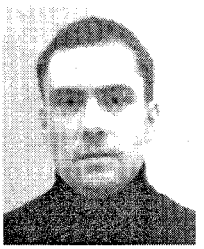

Niels Faché (S'92–M'92) was born July 4, 1964, in Ghent, Belgium. He received the degree in electrical engineering and the Ph.D degree from the University of Ghent, Ghent, Belgium in 1986 and 1989, respectively.

In 1990, he worked as a Consultant from the Laboratory of Electromagnetism and Acoustics (LEA), University of Ghent, to the Network Measurements Division of Hewlett-Packard, Santa Rosa, CA, where he worked on the improvement and implementation of linear models in the Microwave Design System. From 1991 to 1992 he was back with LEA, where he did research on electromagnetic field solvers and their use in circuit simulators. In November 1992, he co-founded Alphabit, a Belgian CAE software company. The company's activities focused on the development of electromagnetic field solvers for the simulation of high frequency circuits. In November 1994 the company was acquired by HP-EEsof (Hewlett-Packard). He is now in charge of the group that develops planar em-technology within HP-EEsof. He has made contributions to more than 30 papers in international journals and conference proceedings. He is also the principal author of one book *Electromagnetic and Circuit Modeling of Multiconductor Transmission Lines* (London: Oxford Univ. Press, 1992).